NBSIR 74-360

A DYE MODE-LOCKED Nd^{+3} GLASS LASER FOR GENERATING ELECTRICAL REFERENCE WAVEFORMS

Tatsutoku Honda
Norris S. Nahman

Electromagnetics Division
Institute for Basic Standards
National Bureau of Standards
Boulder, Colorado 80302
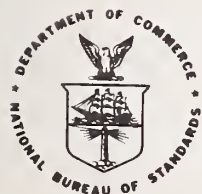
September 1972

NBSIR 74-360

A DYE MODE-LOCKED Nd^{+3} GLASS LASER FOR GENERATING ELECTRICAL REFERENCE WAVEFORMS

Tatsutoko Honda
Norris S. Nahman

Electromagnetics Division
Institute for Basic Standards
National Bureau of Standards
Boulder, Colorado 80302

September 1972

FOREWORD

This report summarizes the research performed by Mr. T. Honda during his stay at the National Bureau of Standards, Boulder, Colorado, as a visiting guest scientist from September 1971 to September 1972. Mr. Honda's home laboratory is the Electrotechnical Laboratory, Tokyo, Japan. This report is typical of the high quality research performed in the international scientific exchange programs that NBS participates in and strongly supports. The major publication from this research was "The Optical Impulse Response of Biplanar Vacuum Photodiodes," coauthored by Mr. Honda and Dr. R. Smith of NBS. The paper was published July, 1973 in Applied Optics.

The second author Dr. Norris S. Nahman was the section chief of the Pulse and Time Domain Section in which Mr. Honda performed his research. Dr. Nahman provided scientific counseling and direction of this research effort. He is no longer with NBS. He is presently the chairman of the Electrical Engineering Department of the University of Toledo, Toledo, Ohio.

James R. Andrews
January 1974

CONTENTS

CONTENTS (Continued)

LIST OF FIGURES

LIST OF FIGURES (Continued)

A DYE MODE-LOCKED Nd^{+3} GLASS LASER FOR GENERATING ELECTRICAL REFERENCE WAVEFORMS

T. Honda* and N.S. Nahman**

The theory, design, construction, operation and stability of dye mode-locked Nd^{+3} glass laser are discussed. Optical properties of a saturable dye, single pulse generation and two-photon fluorescence are experimentally studied. For the application of picosecond optical pulses to the field of the baseband pulse measurements, three types of modelable detectors are described which have possible applications for the generation of electrical reference waveforms.

Key words: Glass laser; laser; mode-lock; Nd^{+3}; picosecond; reference waveform.

1. INTRODUCTION

The purpose of this work was to develop a pulsed laser for generating optical picosecond pulses. The laser is to be used as an optical pulse source in a study on the generation of electrical pulses by optical pulses. A mode-locked Nd^{+3} glass laser was chosen for this work because a glass laser is able to generate the shortest pulses and large peak power [1].

*Mr. Honda was an NBS guest scientist during 1971-72. He is with the Laser Research Section, Radio & Opto-Electronics Division, Electrotechnical Laboratory, Tanashi Branch, Tanashi, Tokyo, Japan.

**Dr. Nahman is presently with the Electrical Engineering Dept., University of Toledo, Toledo, Ohio.

The generation of large output pulses from laser devices was first achieved by McClung and Hellworth [2] in 1962. This technique is now called laser-Q switching; the shortest pulse available from a Q-switched laser is about 10 nsec. By the mode-locking technique it is now possible to produce 0.1 psec pulses [3] at powers up to 100 Gigawatts.

The mode-locked laser pulse generator can be characterized as a regenerative pulse generator. It is well known that a feedback loop consisting of an amplifier, a filter, a delay line and a nonlinear element (which provides less attenuation for a high-level signal than for a low-level signal) behaves as a regenerative pulse generator, figure 1a. In 1955, Cutler [4] discussed the regenerative pulse generator as a microwave pulse generator and was able to generate microwave pulses having 2 ns pulse duration at 4 GHz.

Referring to figure 1a, when the loop-gain exceeds unity, a pulse recirculates indefinitely around the loop and each traversal gives rise to an output pulse at the output terminal. The nonlinear element called an "expandor" by Cutler has the three following characteristics:

1)   Exhibits low loss for the peak region of the re-circulating pulse while a high loss for lower amplitude region.

2)   Discriminates against noise and reflections.

3)   Acts to shorten the pulse duration until the pulse
duration is limited by the inherent bandwidth of the
filter.

The output of the regenerative oscillator has a pulse repetition rate equal to the reciprocal of the loop delay, a pulse duration equal to the reciprocal of the system bandwidth, and a carrier frequency determined by the filter frequency.

A mode-locked laser pulse generator is an optical regenerative pulse generator, figure 1.   The laser medium serves as the amplifier, the combination of the Fabry-Perot resonator and the line width of the laser transition serves as the filter, and the time required for an optical pulse to transverse twice the distance between the mirrors serves as the loop time delay.

The optical analog of the "expandor" is a saturable absorber, such as the reversible bleachable dye solution commonly used in laser Q-switches. The three fundamental requirements for a saturable absorber are as follows:

1)   An absorption line at the laser wavelength.

2)   A line width equal to or greater than the laser line width.

3)   A dye recovery time which is shorter than the loop time delay of the laser.

Such a nonlinear element, figure 2a, sharpens pulses upon repeated traversals of the feedback loop. The pulses become successively peaked until a steady state is reached, figure 2b.

The steady state represents a balance between the narrowing caused by the nonlinear element and the spreading out of the pulse due to the finite line width (frequency bandwidth) of the laser material. The study of short pulse formation in the laser has been approached from two theoretical directions [5-8]. One method is based upon detailed studies of the laser cavity modes [5,7,8]. Such an approach leads to difficult analytical or numerical computation, because of the complicated sets of coupled mode equations. However, such studies have had notable success in explaining short pulses in terms of the locking of the phases of the modes.

The other approach is simpler and is based upon the method used by Cutler in studying microwave pulse generators [4].

The Cutler method of analysis is in terms of functions of time, and it has advantages both in terms of the physical picture and of the mathematical operations involved. Also, the Cutler method of analysis applied by Creighton, et al. [6] is described here because their analysis has rather general forms for the functions representing operations on signal in the laser, whereas most other analyses assume these functions to be Gaussian.

4

2. CUTLER MODEL FOR SATURABLE DYE ABSORBER MODE-LOCKED LASER

2.1 Linear Active Medium

The laser is assumed to be operating on a particular line of central frequency ω_c and approximate width $\delta\omega$, figure 3. A ring laser is imagined to simplify considerations. The light transverses a complete cycle and returns to the input side of the active medium.

Assuming that the active material is not saturated, thus the electric field from it is a linear function of the incident field; also its response is assumed not to vary with time. A linear operator represents both the linear operation of the active medium on the signal, and the lumped losses in the entire optical circuit. The linear operator is taken to have a transfer function $F(\omega)$. Referring to figure 3, if the input signals at A is I(t) and the output signal at B is O(t), then

$$O(t) = \int_{\infty}^{\infty} \overline{I}(\omega) \cdot \overline{F}(\omega) \ e^{-j\omega t} \ d\omega \tag{1}$$

where $\overline{I}(\omega)$ is the Fourier transform of I(t) and $\overline{F}(\omega)$ is the transfer function of the linear operator. From (1)

$$O(t) = \int_{-\infty}^{\infty} F(t-t') \ I(t') \ dt' \tag{2}$$

The response function

$$F(t-t') = \frac{1}{2\pi} \int_{-\infty}^{\infty} \overline{F}(\omega) \, e^{j\omega(t-t')} \, d\omega$$

which has a response time ρ on the order of magnitude of the reciprocal of the bandwidth. $\overline{F}(\omega) \neq 0$ in a narrow range about the optical frequency ω_c. Explicitly in terms of ω_c, $\overline{F}(\omega)$ has the form

$$\overline{F}(\omega) = \overline{M}(\omega-\omega_c) + \overline{M}^*(-\omega+\omega_c) = \overline{M}(\Omega) + \overline{M}^*(-\Omega) \tag{3}$$

$\overline{M}^*$ results from the requirement that linear transfer functions must satisfy the condition $\overline{F}(\omega) = \overline{F}^*(-\omega)$.

If the initial carrier pulse is

$$G(t) = G_{in}(t)\cos \omega_c t \tag{4}$$

and is such that $G_{in}(t)$ varies slowly with respect to the carrier frequency, then the output pulse envelope can be approximated by

$$G_{out}(t) = \int_{-\infty}^{\infty} F(t-t')G_{in}(t') \, dt' \tag{5}$$

which varies slowly compared to optical carrier frequency. We have the approximate result that the filter acts on solely the envelope function as if its transfer function were $\overline{M}(\Omega)$,

$$F(t) = \frac{1}{2\pi} \int_{-\infty}^{\infty} \overline{M}(\Omega)e^{i\Omega t} \, dt \tag{6}$$

6

The width of the response function F(t) is designated by the symbol ρ where ρ^2 is the variance of F(t) (see (11)). The time ρ is long compared to the carrier period, but short compared to the cycle time of the laser.

2.2 Saturable Absorber

Unfortunately, there is no simple way of writing the output from a bleachable dye in terms of its input. The expandor in Cutler's paper was assumed to act on the amplitude of the pulse envelope by a power of S, where S > 1. Although a bleachable dye does not behave in this simple way, it does generally narrow pulses which pass through it as does Cutler's expandor. A pulse going through a laser gives rise to the next pulse; the signal at the output C is

$$G_j^C = \left(\int_{-\infty}^{\infty} F(t-t') G_j^A(t') \; dt' \right)^S \tag{7}$$

where $G_j^A(t)$ is the j-th pulse at the input A. The input for the (j+1) pulse is

$$G_{j+1}^A(t) = \left(\int_{-\infty}^{\infty} F(t-T_{CA}-t') G_j^C(t') \; dt' \right)^S \tag{8}$$

2.3 The Steady State

The steady state condition is given by

$$G(t-\Delta') = \left(\int_{-\infty}^{\infty} F(t-t') G(t) \; dt' \right)^S = G(t) \tag{9}$$

7

where

$$\Delta' = T_{AC} = T - T_{CA} \tag{10}$$

Here T is the total time for a pulse to travel around the loop; T_{AC} is the time for travel from A to C, while T_{CA} is that for C to A.

For a criterion for the pulse duration, we use the variance defined by

$$V_f = \frac{\int_{-\infty}^{\infty} (t-<t>^2) f(t) \, dt}{\int_{-\infty}^{\infty} f(t) \, dt} \tag{11}$$

where

$$<t> = \frac{\int_{-\infty}^{\infty} t f(t) \, dt}{\int_{-\infty}^{\infty} f(t) \, dt}$$

This is a convenient criterion because variances add under convolution, i.e., for

$$f(t) = \int_{-\infty}^{\infty} g(t-t')h(t') \, dt', \tag{12}$$

we have

$$V_f = V_g + V_h \tag{13}$$

From (9) we have

$$G(t-\Delta')^{1/S} = \int_{-\infty}^{\infty} F(t-t')G(t') \, dt'$$

8

Furthermore, if G(t) is a Gaussian function, then the variance for $G(t)^{1/S}$ is the variance of G(t) multiplied by S. Denoting the variances of G(t) and F(t) by σ^2 and ρ^2, respectively, then

$$\sigma^2 = \frac{\rho^2}{S - 1}, \tag{14}$$

where $\rho \simeq \frac{1}{\delta\omega}$ (approximately the lifetime of the gain medium line). When S = 2, we have a square law saturable absorber and (14) reduces to

$$\sigma = \rho \simeq \frac{1}{\delta\omega}, \tag{15}$$

which says that the pulse width ρ is approximately equal to the reciprocal of the gain line bandwidth. Cutler's analysis [4] yields a similar result.

In the case of a Gaussian filter function and pulse shape, and a square law saturable absorber, Cutler finds for the pulse duration,

$$\tau = \frac{8/\pi}{\Delta\omega} \left[\frac{\left(1 + \frac{\gamma^2 \Delta\omega^4}{16}\right)}{1 + \left(1 + \frac{\gamma^2 \Delta\omega^4}{18}\right)^{1/2}} \right]^{1/2} \tag{16}$$

where γ is the coefficient for the nonlinear effect originating from the dispersion, and $\Delta\omega$ is the bandwidth for a Gaussian filter defined by the response at the minus-one neper points. If γ is small enough,

$$\tau = \frac{4/\pi}{\Delta\omega}, \tag{17}$$

which is the same form as (15).

3. DYE MODE-LOCKED Nd^{+3} GLASS LASER [9], [11]

3.1 Geometry

A schematic diagram of the dye mode-locked laser is shown in figure 4. The laser produces an output at 1.06 µm which is invisible and in the infrared range. The laser glass rod is 1.6 cm in diameter and 19.3 cm in length; the rod is brewster cut at both ends; and made of Nd^{+3} doped laser glass. The laser rod is housed in the center of a double elliptical pumping cavity having a gold-polished surface, containing two straight Xenon lamps. 14.5 cm of the laser rod is in the pumping cavity. The mirrors are wedged and anti-reflection coated on the back surfaces at 1.06 µm. In some experiments, we used an output mirror having a lower reflectivity of 60% in order to change the threshold of lasing. Also the other mirror had a radius of curvature of 10 m to form a stable resonator. The saturable dye (9860) is housed in a thin cell constructed with a 1.65 mm PTFE spacer; the dye was dissolved in 1,2-dichloroethane and the transmission adjusted to be 75 to 80 percent. The dye was put in close proximity to the 100% mirror [12]. The laser emission shown in figure 5 is observed with a photodetector (Biplanar Vacuum Photodiode) and a traveling-wave oscilloscope (over all rise-time 0.55 nS). It has the form of a train of approximately 50 short pulses spaced by about 10 ns, the cycle time T of the laser.

10

3.2 Pump Energy Charging and Discharging Circuit

The block diagram of the laser flashlamp pumping system is shown in figure 6. The capacitor bank consists of ten capacitors of 25 μf parallel connected so as to store 1000 joules when a charging voltage of 2.8 kV is applied. The Xe lamp is triggered in a series mode [13] by using a pulse transformer having a saturable inductance, which also serves as a current limiter.

4. OPERATION OF THE Nd^{+3} GLASS LASER

4.1 Alignment of the Laser System

Alignment of the system initially is done by using the
visible beam of a cw He-Ne laser (0.6 μm) as a "guiding-
string." It is rather hard to make a good alignment using
a simple serial alignment on the He-Ne beam. A better proce-
dure is to employ a Fabry-Perot interference pattern from the
incident side of the resonator where the screen on which the
pattern images is kept as far as possible from the resonator.
The reflected beams from the mirrors should be completely
superimposed by adjusting mirrors while watching the inter-
ference pattern. However, it should not be expected that
the alignment will be perfect before lasing because the lasing
wavelength (1.06 μm) will be different from that of the He-
Ne beam (0.6 μm). The final adjustments must be made under
actual lasing conditions. The actual far-field pattern
will show whether or not the alignment has been done
correctly and is obtained from burn patterns produced by
the laser beam, figure 7.

4.2 Concentration of Absorber Dye

The dye 9860 was chosen as a saturable absorber for mode-
locking because it has some advantages involving high satura-
tion power density, fast relaxation time and high damage
threshold, table 1.

12

For determination of the dye concentration, it is necessary to consider the excitation energy capacity and optical damage threshold of the rod and mirrors. Too high a concentration of dye makes the lasing threshold of a mode-locked laser too large; this in turn could require optical energy stored inside the laser to be equal to or larger than the optical damage threshold.

In the case of too low concentration of dye, the laser would be poorly mode-locked.

4.3 Excitation Energy

Usually, excitation level is determined by a "cut and try" method. The threshold of a mode-locked laser depends upon the gain and losses of the whole laser system involving the reflectivity of mirrors and the absorption of the dye.

It is necessary to avoid pumping near the threshold, because too low pumping causes instability of lasing and mode-locking, and is strongly influenced by the fluctuation of the excitation power from Xenon lamps which can be 10 to 20 percent. Too high a pumping level can cause damage to the laser components. Consequently, care must be taken in increasing the pumping level to achieve stable operation.

4.4 Optical Damage

Optical damage on the surfaces of optical devices such as mirrors and in bulk materials such as rods can be produced by high power mode-locked laser pulses. The surface damage results from optical power absorbed at dirty spots on surfaces of optical devices. Surfaces should always be kept clean.

In bulk materials an excessively high power laser beam can lead to self-focusing of the optical beam. To avoid the production of "hot-spots" in the beam uniform pumping and homogeneous dye solution are required.

4.5 Time Interval of Operation

The shot to shot time interval allowed depends on the cooling time constant of an overall system and pumping energy level. Generally speaking, regular (periodic) operation results in a good reproducibility of lasing; however, the repetition rate must be slow enough so that the system cools down to the same initial state. Typical repetition rates would be of the order one shot/10 minutes for highest power operation.

5. STABILITY OF DYE MODE-LOCKED LASER

Instability of a dye mode-locked laser is caused by various conditions of the components in the laser system. The main causes which impede stability of mode-locked laser and the appropriate counter-measures are shown in table 2. The detail about some of these causes will be discussed below. A typical example of shot to shot instability of dye mode-locked laser is shown in figure 8.

5.1 Laser Rod

The pumping energy heats the laser rod and produces a temperature gradient throughout the rod. This gives rise to a change of refractive index and mechanical distortion in the rod if the distribution of pumping energy and absorption is not uniform.

It is well known that glass is a poor thermal conductor. It will take a considerable amount of time until the heated rod will cool. For a simple estimation of the thermal diffusivity, we have to take into account a thermal time constant of about 30 to 50 sec for the glass material. If an energy of 100 joules (equivalent to electrical input energy of 1000 joules applied to Xenon lamp of 10% efficiency) is absorbed by the glass rod, the temperature would correspondingly rise by 1.6 to 2.6°C.

5.2 Excitation

An example of excitation energy dependence of mode-locking is shown in figure 9. From these pictures, the mode-locking threshold can be observed.

By observing the intensity of 0.53 μm emitted from a Xenon lamp, a shot to shot intensity fluctuation of 10 to 20% was found. The fluctuation is influenced by the change of charging voltage, triggering, and physical situation of the lamp. The electrically induced fluctuation troubles may be minimized by utilizing an electronic automatic and internal (series) triggering method for driving the Xenon lamps.

The physical situation of the lamp is complicated. The emission around 0.58 μ is most effective for lasing; however, the spectrum emitted from a Xenon lamp depends upon temperature, pressure, input energy and use-degradation of the lamp. Over-all, better shot to shot energy stability can be achieved by regular operation at not too low a discharging voltage.

5.3 Degradation of the Bleachable Dye

It has been noted that the dye solution dominates the stability of a saturable absorber mode-locked laser. Unfortunately, only experience can provide the information for establishing the generation of good mode-locked pulses.

The dye manufacturer suggests that the life of dye is about 500 shots at optical power level of 1 to 5 MW. This power level seems to be quite low for the laser system discussed here. Experimentally poor mode-locking has been observed after 30 to 60 shots, figure 10. The degradation of the dye solution results in the change of its transmission property, which destroys mode-locking. If the dye solution loses its essential optical nonlinearity, no mode-locking can be achieved.

The transmission property of a dye can be measured by transmission experiments. The intensity dependence of the optical absorption for a dye solution was measured by using a train of short pulses from a mode-locked laser. A block diagram of the measurement system is shown in figure 11.

To obtain an appropriate optical power density for bleaching the dye, a lens having a focal length of 50 cm was used. A dye cell 1.65 mm thick was placed away from the lens by about 30 cm in order to give approximately the same optical power density as that stored in the mode-locked laser. The laser beam is split into two beams; one is used as a reference and the other as the probe. The test cell has the same size as one being used for mode-locking. Both beams are detected by a vacuum photodiode (0.5 ns risetime) and the output pulses are displayed by a traveling wave oscilloscope (0.35 ns risetime).

The intensity dependence of the optical absorption of the 9860 dye solution is demonstrated in figure 12; less absorption at high power can be seen. The results of the transmission measurements on the 9860 dye solution are shown in figure 13. The solid-line curves are theoretical ones computed by using the two-level model developed by Hercher [14].

For a thin cell mode (propagation through the cell < optical pulse duration), Hercher gives for the transmission, T,

$$T = 1 - \frac{a_o}{I/I_S},$$

where a_o is the small signal absorption, and I_S is the optical intensity at which absorption is $a_o/2$.

The small signal transmission was measured separately by using a combination of a white spectrum lamp, a spike (transmission) filter for 1.06 µm and a photomultiplier. The small signal transmission was adjusted to 37.5%, 62.5%, and 78%. The curves of the thin cell model account well for the experimental points for the weak absorbing dye solution. The two-level model has been supported experimentally [15]. As noted by the ref. [15], we have also observed a decrease of the transmission for optical pulse intensities larger than a certain value.

In figure 14, the change in the transmission property for a 9860 dye solution resulting from mode-locked laser operation is shown. Apparently the nonlinearity of the dye was weakened. The dye solution was degraded in the mode-locked laser after 35 shots; note the increase in the small signal transmission. The degraded dye could no longer provide the necessary mode-locking nonlinearity.

In this case, the number of shots of mode-locking operation is not so important, but rather the change of the transmission property of the degraded dye solution when it happened. It should be also noted that the excitation power for mode-locked lasing with fatigued dye is lower than with new dye.

Also the transmission property of dye solution is strongly influenced by absorption of blue light and ultra-violet radiation. The change of the small signal transmission of the dye solution versus exposure time under a fluorescent lamp is shown in figure 15. The completely bleached out state of the dye is shown. It may be concluded that the degradation of dye could be considerably influenced by blue and ultra-violet light from Xe lamps.

6. SINGLE PULSE EXTRACTION AND MEASUREMENT

6.1 Pulse Extraction

A single pulse can be extracted from a train of pico-
second pulses by using an optical gate, figure 16. The gate
consists of an electrooptical polarization switch placed be-
tween two polarizers. When the gating pulse is applied to
the polarization switch, the polarization of the optical
signal is changed; consequently, if the signal is then passed
through a polarization discriminator, the signal will be
spatially separated into its two distinct polarization
components. The gating pulse of 4 to 5 kV, 8 to 10 ns is
generated by a spark gap pulse generator which is triggered
by the laser beam. A typical picture of single pulse genera-
tion is shown in figure 17.

A single picosecond pulse is considered to be very useful
for electrical time domain studies. Furthermore, this tech-
nique makes it possible to obtain the single pulse having the
shortest duration in the train of optical pulses.

6.2 Two Photon Fluorescence Pulse Measurements

Optical coincidence techniques involving intensity auto-
correlation functions have been very useful in the study of
ultrashort optical pulses of a few picoseconds in duration.

A commonly used technique is that of two photon fluorescence
(TPF) [16]; the block diagram for a TPF measurement of pulse
width is shown in figure 18. The laser beam is divided into
two beams of equal intensity; these interfere in a dye which
exhibits two-photon induced fluorescence. The pulse duration
is proportional to the width of the auto-correlation function.

The time-integrated fluorescence intensity F(t) excited
by the two identical wave packets V(t) propagating in the
opposite direction is given in terms of the correlation
function $G^2(\tau)$:

$$F(t) = 2F_0[1+2G^2(\tau)/G^2(0)]$$

in which

$$G^2(\tau) = <V(t)V(t+\tau)> <V^*(t)V^*(t+\tau)>$$

where $\tau = 2Z/V_g$ (V_g = group velicty of the wave packets and Z is the
position) and F_0 the single pass fluorescence. The notation
$<V(t)V(t+\tau)>$ denotes the integration

$$\lim_{T\to\infty} \frac{1}{T} \int_{-T/2}^{T/2} V(t)V(t-\tau)\ dt$$

The contrast ratio K of the fluorescence pattern is de-
fined as the ratio of the peak fluorescence at $\tau = 0$ to the
background fluorescence at large values of τ;

$$K = F(0)/F(\tau\to\infty)$$

It is well known that K assumes the value of 3 in the absence
of background intensity and reduces to 1.5 for Gaussian noise
which is caused by the thermal radiation generated by a laser
beam.

Rhodamine 6G was utlized as the dye medium. In ethanol solution, this dye has its primary absorption peak at a wavelength that is quite close to the 0.53 μm, the second harmonic of the Nd^{+3} glass laser. In figures 19 and 20, some typical pictures of TPF by mode-locked pulses are shown.

For TPF experiments, it is always necessary to adjust carefully the optical beams to be completely superimposed in optical power density. Too strong optical power increases noise and reduces the contrast ratio.

The two-photon fluorescence method has considerable ambiguity for determinating pulse duration because the pulse waveform is unknown. Many workers have been trying to find the waveform of mode-locked pulses and measure these pulse duration. It is said that the front part of a mode-locked pulse is expressed with Gaussian and the tail exponential.

In spite of the ambiguity of TPF, the method is very useful for the estimation of picosecond pulse duration because of its simplicity and one shot measurement capability.

7. GENERATION OF ELECTRICAL PULSE WAVEFORM OF KNOWN SHAPE

7.1 Introduction

In the NBS Section 272.20, research has been done on reference waveform generators and standards [17] to be used in pulse measurements and other applications. The method employs the band-limiting properties of a lossy uniform transmission line to produce a known waveform and generator impedance. An example of generator design employing planar skin effect metal loss and debye dielectric loss with a unit ramp generator is shown in figure 21a.

The ultimate application of the laser system described in this report is to replace the convolution problem of the combination of a unit ramp generator and a modeled line by the combination of a picosecond optical pulse generator and a modeled detector, figure 21b.

Three kinds of optical detectors have been considered for the modeled detector having a predictable impulse response: 1) fast thermal photodetector; pyroelectric effect, 2) biplanar vacuum photodiode, and 3) nonlinear optical effect: optical rectification.

7.2 Pyroelectric Detector

The pyroelectric effect [18, 21] concerns the change in the polarization of a polar crystal when it undergoes a variation in its temperature. Optical radiation is absorbed

23

by means of a surface block of an optically absorbing material attached to a piece of spontaneously polarized pyroelectric material. If the pyroelectric material serves as the dielectric in a capacitor, then the resultant change of polarization due to heating of the pyroelectric gives rise to a pyroelectric voltage across the capacitor electrodes.

The fast thermal photodetector is expected to generate an electrical pulse waveform having a risetime of 100 picoseconds. The pyroelectric current is given by,

$$i_p = AP \frac{dT}{dt}$$
$$= \frac{P\Delta\overline{W}}{pCb}$$

where $P = \frac{dP_s}{dT}$, P_s: spontaneous polarization, T: temperature, C: specific heat, b: thickness of pyroelectric material, A: area of detector, $\Delta\overline{W}$: change of radiation power, p: density of pyroelectric material. An equivalent circuit is shown in figure 22. The output voltage V_o is given by

$$V_o = kI_o \left(\frac{1}{T_T} - \frac{1}{T_e} \right)^{-1} \left(e^{-\frac{t}{T_e}} - e^{-\frac{t}{T_t}} \right)$$

where T_T is thermal time constant, T_e circuit time constant ($R_L C$), and I_o peak intensity.

In figure 23, the output signals to be expected are shown for the pyroelectric detection process in cases of both impulse and step incident optical beams. Generally, this detector has a

24

disadvantage of small signal output. An example of pyroelec-
tric photodetector design is shown in figure 24. Ni film
electrodes of 200 Å thick were evaporated on both surfaces
of a PVF$_2$ pyroelectric film of $\simeq$ 100 μm thick.

7.3 Biplanar Vacuum Photodiode

The impulse response of a biplanar vacuum photodiodes
[22, 24] was experimentally investigated [27] by the use of
a single ultrashort laser pulse from a train of mode-locked
pulses. The impulse response of a biplanar vacuum photodiode
for the observation of ultrashort optical pulses is determined
by the transit time of the photoelectrons from the photocathode
to the anode, figure 25.

Transit time of a photoelectron traveling across the
distance between electrodes is given by

$$T = d\sqrt{\frac{2m}{eV}}$$

The photocurrent is written as

$$i_p = Q\,\frac{v}{d}$$

where v = velocity of charge, Q = total photoelectron charge,
and

$$v = \frac{2d}{T^2}\,t.$$

25

The equivalent circuit for the biplanar diode is shown in figure 26. The output voltage V_o is

$$V_o = \frac{2Q}{T^2}\left[t - \tau(1-e^{-\frac{t}{\tau}})\right], \quad 0 \le t \le T$$

$$V_o = \frac{2Q}{T^2}\left[T - \tau(1-e^{-\frac{T}{\tau}})\right]e^{-\frac{(t-T)}{\tau}}, \quad T < t$$

where $\tau = RC_p$. A graph of V_o is shown in figure 27. By the use of the planar vacuum photodiode, it is possible to generate electrical pulses having large peak voltages with risetime of 100 ps.

7.4 Optical Rectification

The nonlinear optical effect induced by a strong optical beam in a crystal has a component of DC electrical polarization; the production of the electrical polarization is called optical rectification [25, 26]. The DC polarization induced by light is given by

$$Pi(0,1\gamma) = X_{2ijk}(0,\omega-\omega)\ \underline{E_j(\omega,1\gamma)E_k^*(\omega,1\gamma)},$$

that is, proportional to optical power. The induced current is represented by

$$i_{or} = \frac{dP}{dt} = X_2\frac{dI}{dt}$$

where P is the integrated polarization over the volume of a crystal and I is optical power. Typical materials available

26

for the optical rectification are KDP, ADP, $LINbO_3$ and $LiNbO_3$, etc. each of which lack the inversion symmetry in the crystal structure. The broadband response of the optical rectification effects coupled with an appropriate transmission line and intense picosecond laser pulses suggests the use of the effect for generating picosecond electrical pulses.

ACKNOWLEDGMENT

by T. Honda

REFERENCES

[1] A.J. DeMaria, W.H. Glenn, Jr., M.J. Brienza, and M.E. Mack, "Picosecond Laser Pulses," Proc. IEEE, Vol. 57, No. 1. pp. 2-25, January 1969.

[2] F.T. McClung and R.W. Hellwarth, "Gaint Optical Pulses from Ruby," J. Appl. Phys., Vol. 33, pp. 828-829, March 1962.

[3] R.W. Smith, "Mode-Locking of Lasers," Proc. IEEE, Vol. 58, No. 9, pp. 1342-1357, September 1970.

[4] C.C. Cutler, "The Regenerative Pulse Generator," Proc. IRE, pp. 140-148, February 1955.

[5] S.E. Schwarz, "Theory of an Optical Pulse Generator," IEEE J. Quantum Electronics, Vol. QE-4, No. 9, pp. 503-514, September 1968.

[6] J.R. Creighton and J.J. Jackson, "Simplified Theory of Picosecond Pulses in Lasers," J. Appl. Phys., Vol. 42, No. 9, pp. 3409-3414, August 1971.

[7] N.G. Bosov, P.G. Kriukov, V.S. Letokhov, and Y.V. Senatskii, "H-12-Generation and Amplification of Ultrashort Optical Pulses," IEEE J. Quantum Electronics, Vol. QE-4, No. 10, pp. 606-609, October 1968.

[8] D.J. Kuizenga and A.E. Siegman, "FM and AM Mode-Locking of the Homogeneous Laser -- Part I: Theory," pp. 694-708, "Part II: Experimental Results in a Nd: YAG Laser with Internal FM Modulation," pp. 709-715, IEEE J. Quantum Electronics, Vol. QE-6, No. 11, November 1970.

[9] K. Patek, "Glass Laser," London Iliffe Books.

[10] M.A. Dugvay, et al., "Study of the Nd: Glass Laser Radiation," IEEE J. Quantum Electronics, Vol. QE-6, pp. 725-743, November 1970.

[11] D. Von Der Linde, "Experimental Study of Single Picosecond Light Pulses," IEEE J. Quantum Electronics, Vol. QE-8, No. 3, pp. 328-338, March 1972.

[12] E.M. Garmier and A. Yariv, "Laser Mode-Locking Saturable Absorbers," IEEE J. Quantum Electronics, Vol. QE-3, No. 6, pp. 222-226, June 1967.

[13] W.R. Hook, et al., "Xenon Flashlamp Triggering for Laser Application," IEEE Transaction on Electron Devices, Vol. ED-19, No. 3, pp. 308-314, March 1972.

[14] M. Hercher, "An Analysis of Saturable Absorbers," Applied Optics, Vol. 6, No. 5, pp. 347-954, May 1967.

[15] A. Penzkofer, et al., "The Intensity of Short Light Pulses Determined with Saturable Absorbers," Optics Communication, Vol. 4, No. 5, pp. 377-379, January 1972.

[16] J. A. Giordmaine, et al., "Two-Photon excitation of fluorescence by picosecond light pulses," Appl. Phy. Lett., Vol. 11, pp. 216-218, October 1967.

[17] W.D. McCaa, Jr., and N.S. Nahman, "Generation of Reference Waveforms by Uniform Lossy Transmission," IEEE Transaction on Instrumentation and Measurement, pp. 382-390, Vol. IM-19, No. 4, November 1970.

[18] E. Fatuzzo and W.J. Merz, Ferroelectricity, John Wiley & Sons, 1967, pp. 63-76.

[19] J.R. Alday, "Millimeter Wave Detectors Using the Pyroelectric Effect," IEEE Trans. on Electron Devices, Vol. ED-16, No. 6, pp. 598-601, June 1969.

[20] R.A. Cowley, et al., "Dielectric Response in Piezoelectric Crystals," J. Physics-C, Vol. 4, No. 10, pp. L-203, July 1971.

[21] M. Simhony and A. Shavlor, "Pyroelectric Voltage Response to Step Signals of Infrared Radiation in Triglycine Sulphate and Strontium Barium Niobate," J. Appl. Phys., Vol. 42, No. 10, pp. 3741-3744, September 1971.

[22] L.K. Angerson and B.J. McMurtry, "High Speed Photodetectors," Proc. IEEE, Vol. 54, No. 10, pp. 1335-1349, October 1966.

[23] H. Melchior, M.B. Fisher, and F.R. Arams, "Photodetectors for Optical Communications Systems," Proc. IEEE, Vol. 58, No. 10, pp. 1466-1486, October 1970.

[24] P.J.R. Laybourn, "Photodetectors for Laser Application," Optics and Laser Technology, pp. 76-82, 1971.

[25] M. Bass, P.A. Franken, J.F. Ward and G. Weinreich, "Optical Rectification," Phys. Rev. Letters, Vol. 9, No. 11, pp. 446-448, December 1962.

[26] M.J. Brienza, A.J. DeMaria, and W.H. Glenn, "Optical Rectification of Mode-Locked Laser Pulses," Physics Letters, Vol. 26A, No. 8, pp. 390-391, March 1968.

[27] R.L. Smith and T. Honda, "The Optical Impulse Response of Biplanar Vacuum Photodiodes," to be published.

Table 1   PROPERTIES OF MODE-LOCKING DYES

DYE	9740	9860
ABSORPTION PEAK	1.045 μm	1.051 μm
SATURATION POWER DENSITY	40 MW/cm^2	50 MW/cm^2
RELAXATION TIME*	25 $\sim$ 35 X 10^{-12} Sec	6 $\sim$ 9 X 10^{-12} Sec
DAMAGE THRESHOLD (Relative Unit)	15	43

Table 2

MAIN CAUSES WHICH DESTRUCT STABILITY OF
MODE-LOCKED LASER

COUNTERMEASURES

1. MECHANICAL:

    RESONATOR (MISALIGNMENT)

    VIBRATION FREE, STABLE TABLE
    MONITORING OPTICAL ALIGNMENT

2. THERMAL:

    LASER ROD (THERMAL DISTORTION)

    COOLING (REGULAR OPERATION)

3. OPTICAL:

    POOR QUALITY OF LASER ROD AND
    MIRRORS, FLUCTUATION OF Xe LAMP,
    DAMAGE OF DEVICE

    RATE OF LAMP, CONSTANT EXCITATION ENERGY

4. ELECTRICAL:

    DISCHARGING AND TRIGGERING
    TROUBLE

    ADJUSTING CIRCUIT PARAMETER, USING SERIES
    TRIGGERING

5. CHEMICAL:

    DEGRADATION OF DYE

    CIRCULATING DYE SYSTEM

6. OTHERS:

    DUST ON SURFACES OF DEVICES

    CLEAN GAS FLOWING
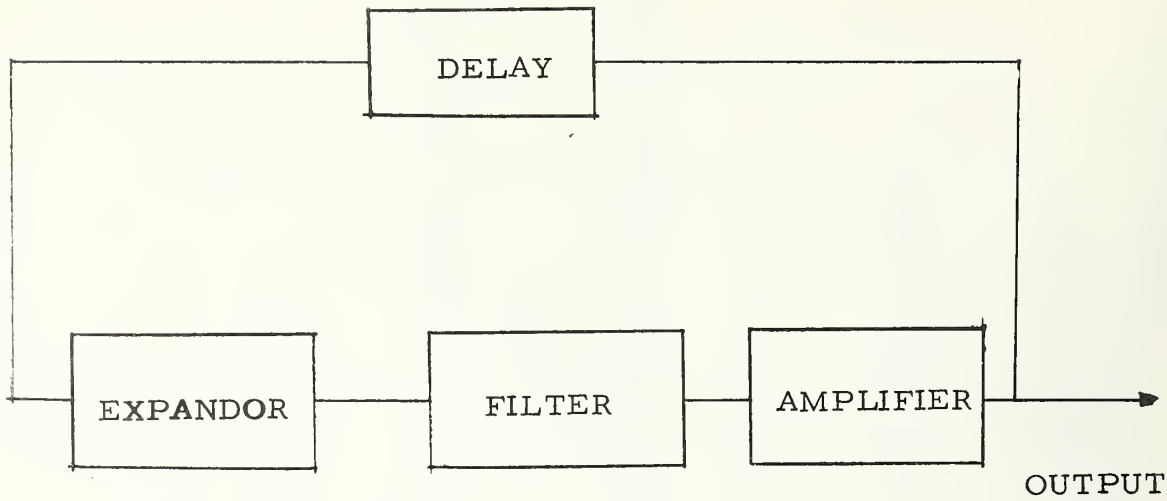
(a) System Model.
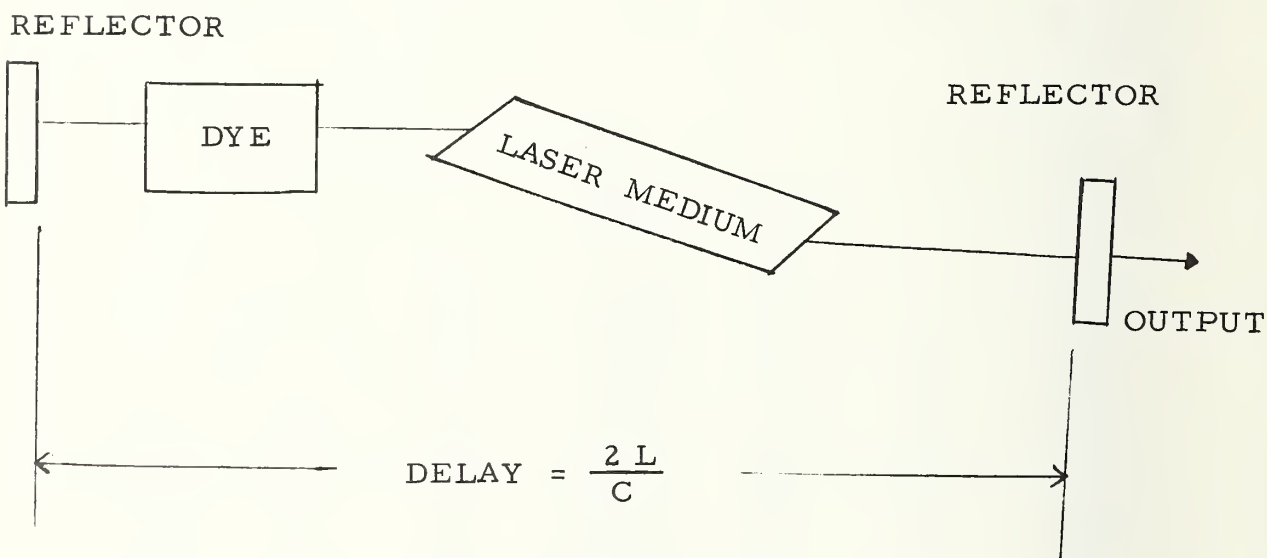
(b) Laser Pulse Generator.

$$DELAY = \frac{2L}{C}$$

Figure 1   A MODEL FOR ELECTRONIC AND OPTICAL
REGENERATIVE PULSE GENERATORS.

$$\alpha = \frac{\alpha_o}{1 + \frac{I}{I_s}}$$
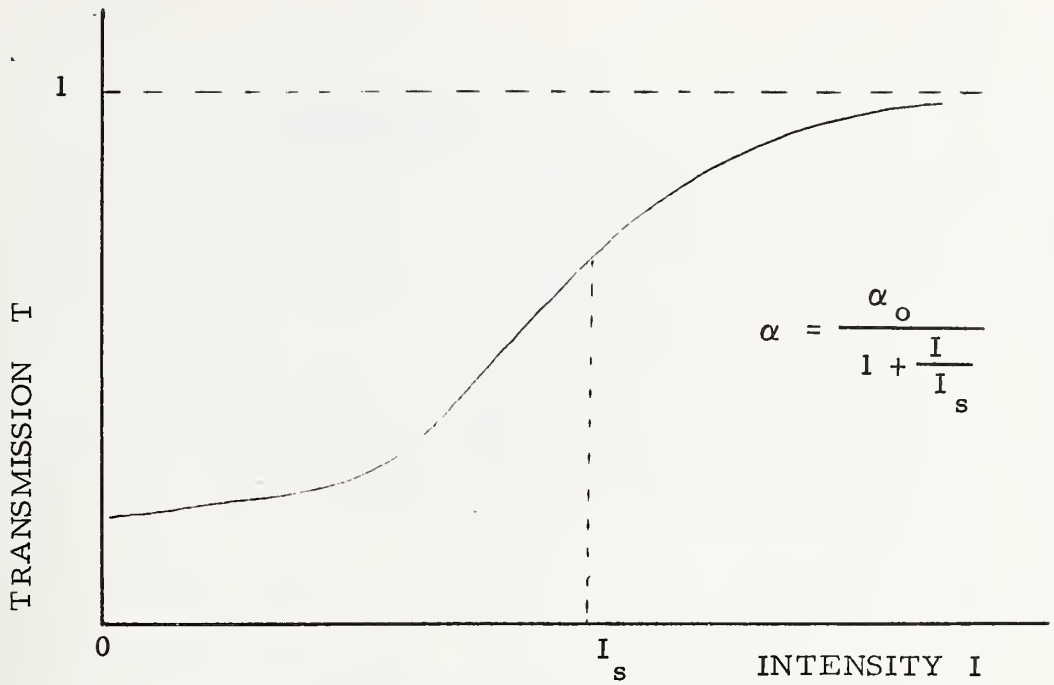
Figure 2a OPTICAL NONLINEAR ELEMENT FOR
MODE LOCKED LASER.

NUMBER OF PASSES

G = 1.4

T = 0.7

Gaussian Pulse
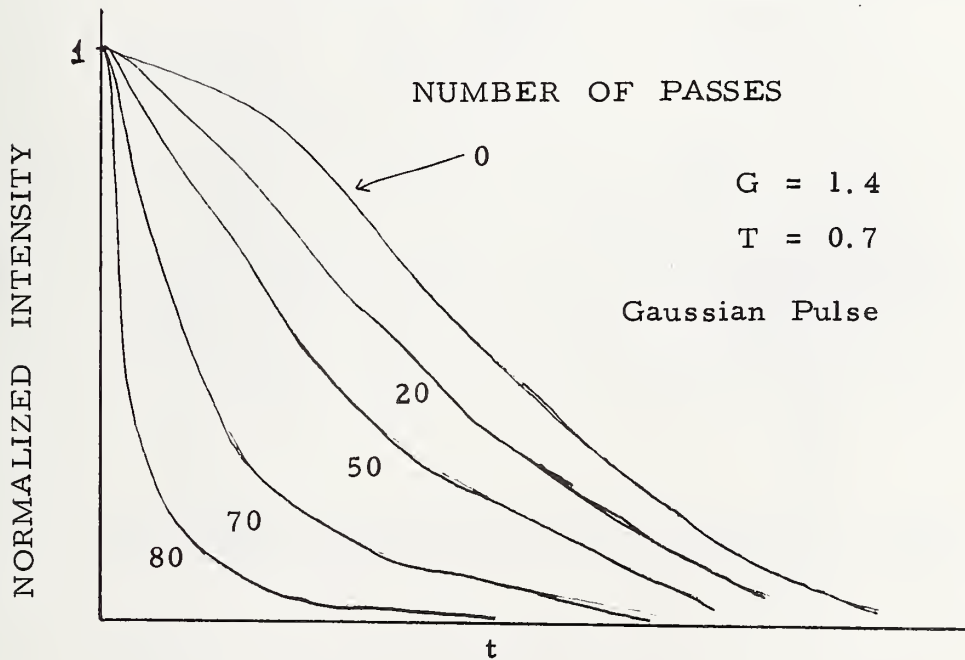
Figure 2b PULSE SHARPENING DUE TO REPEATED
TRAVERSALS OF THE FEEDBACK LOOP.
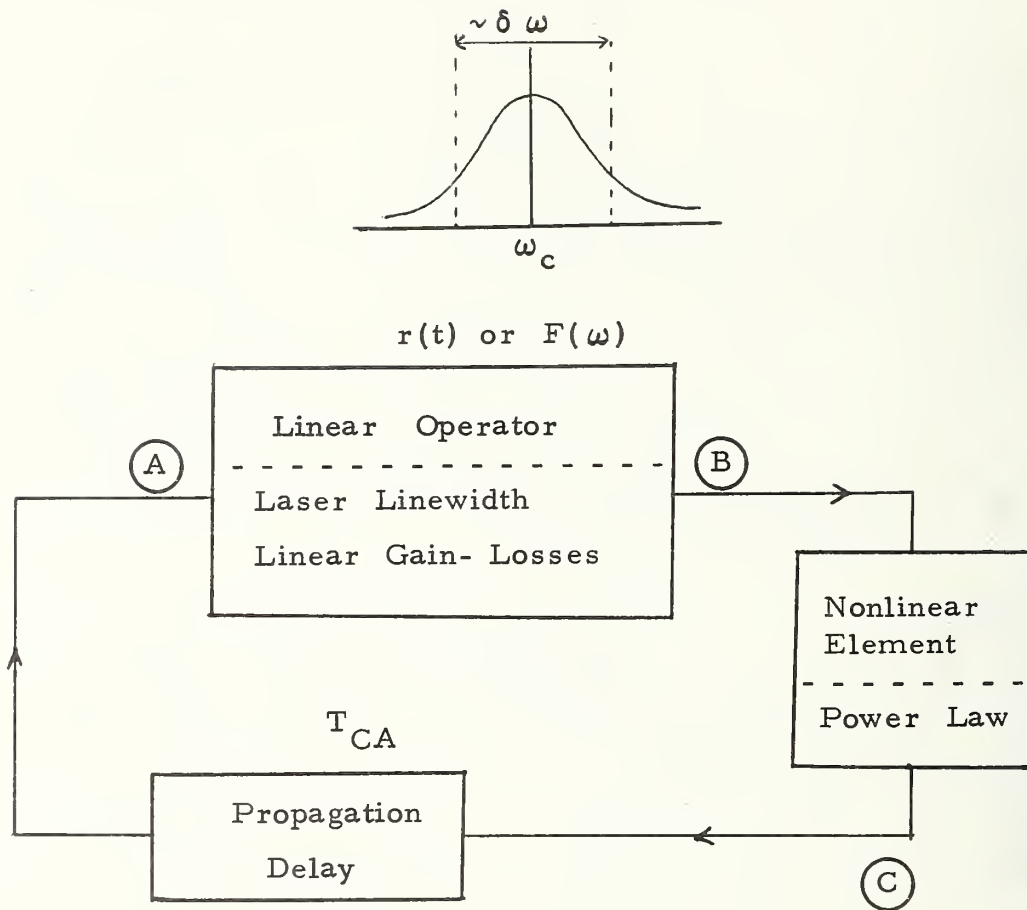
Figure 3 LASER MODEL FOR CUTLER ANALYSIS.
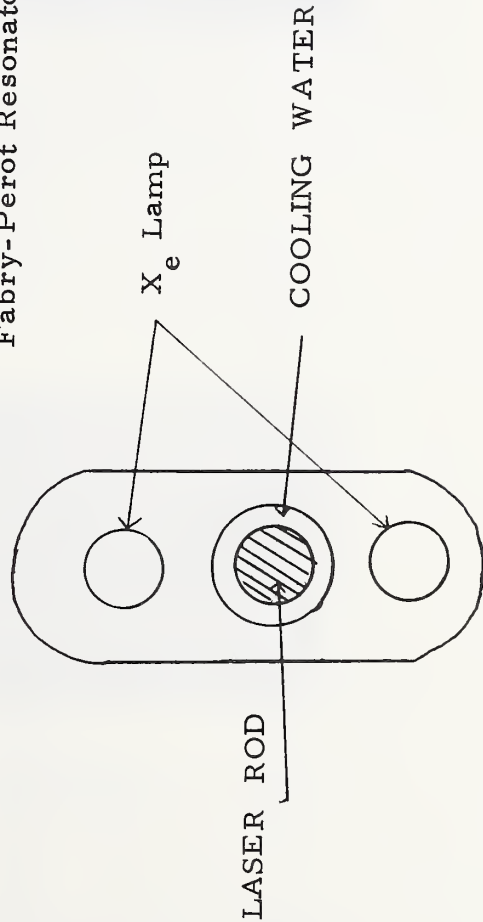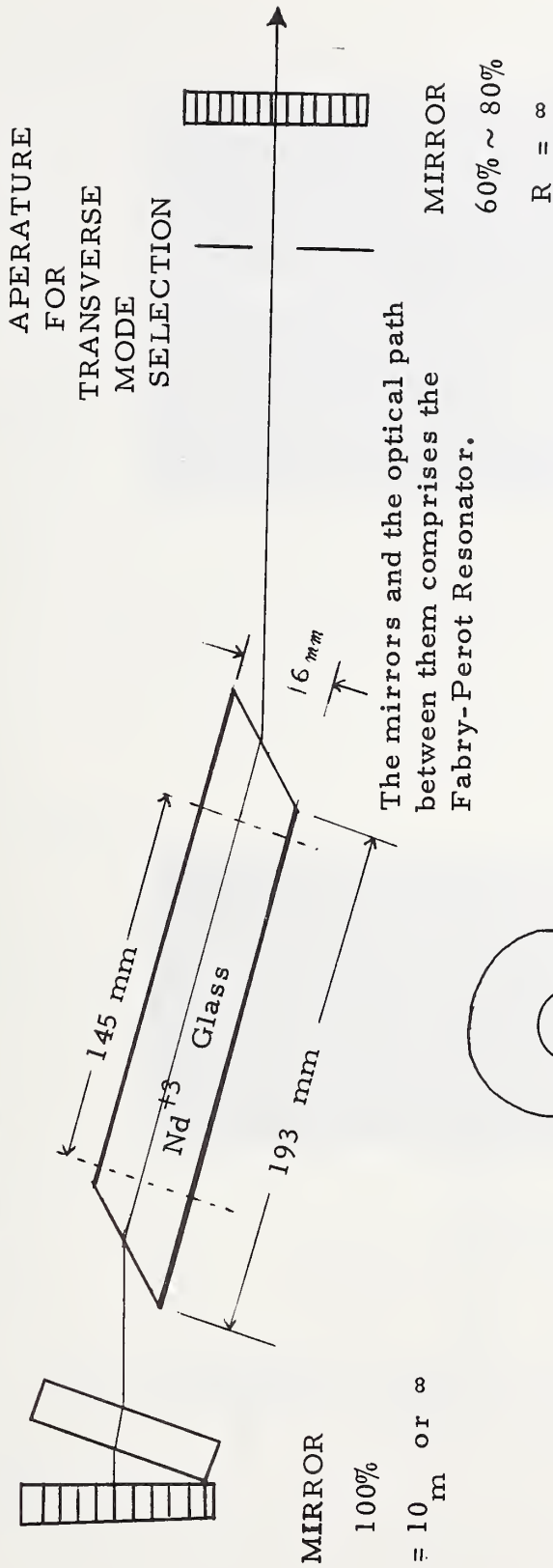
Figure 4   MODE LOCKED Nd^{+3} GLASS LASER

37
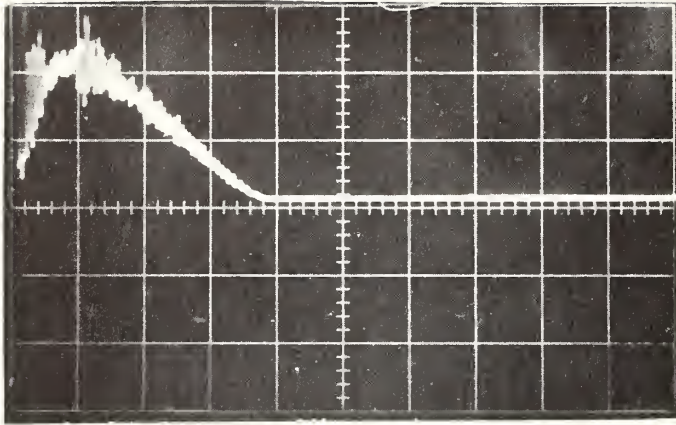
200 μs/ div
Conventional
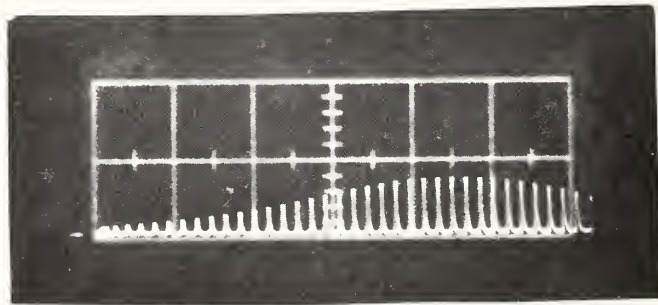
50 ns/div
dye mode-locked

Figure 5   CONVENTIONAL LASER AND MODE
LOCKED LASER OUTPUTS.
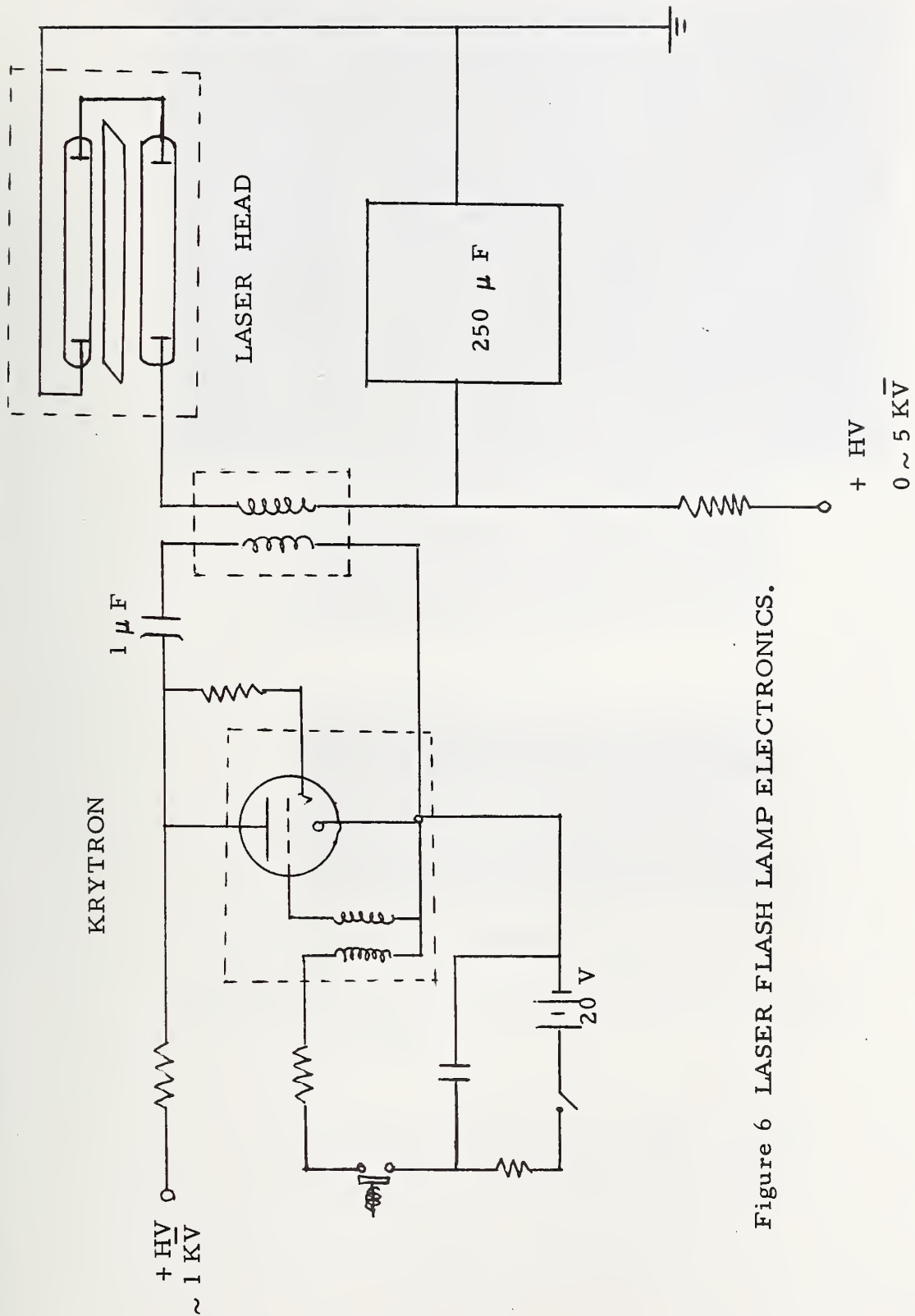
Figure 6 LASER FLASH LAMP ELECTRONICS.

39
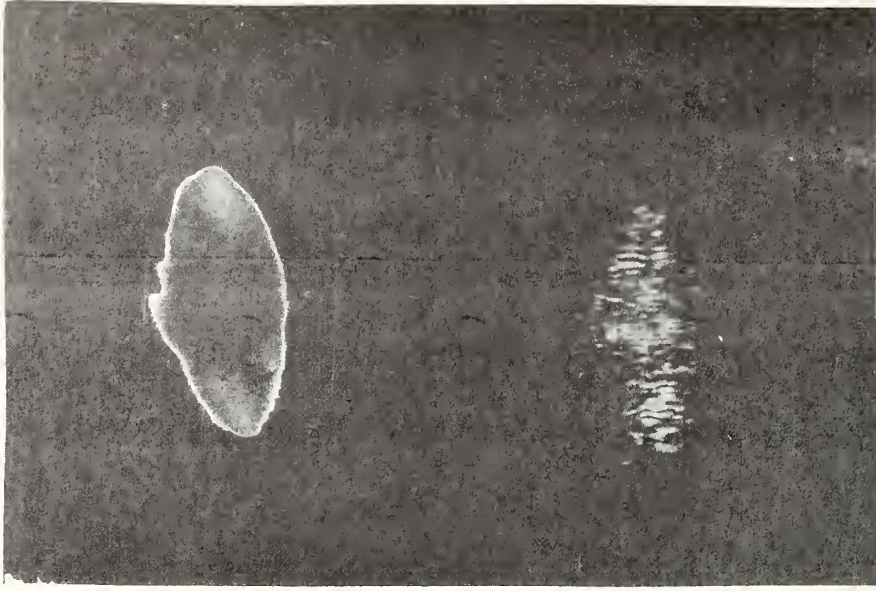
Conventional   Mode-locked

Figure 7   LASER BURN PATTERNS.
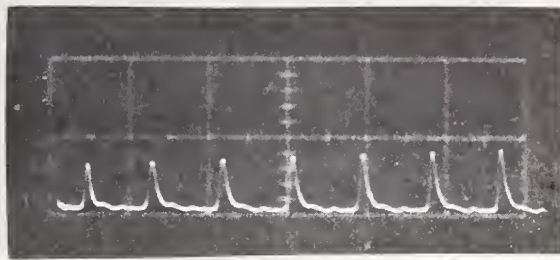
Shot #1
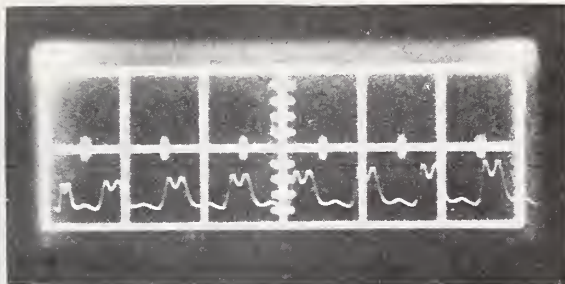
Shot #2
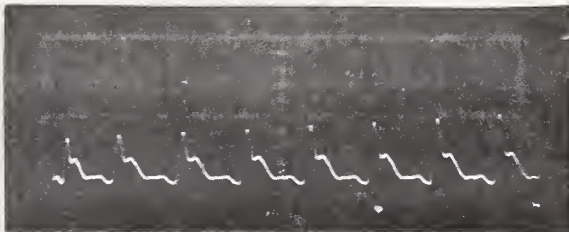
Shot #3

Figure 8   SHOT TO SHOT INSTABILITY OF MODE
  LOCKING.

9860 dye(T=80%), 100% & 70% mirrors,

800J constant, time scale = 10 ns/div.

41
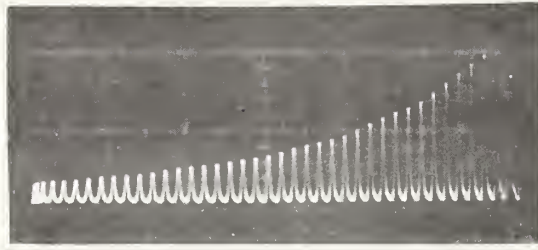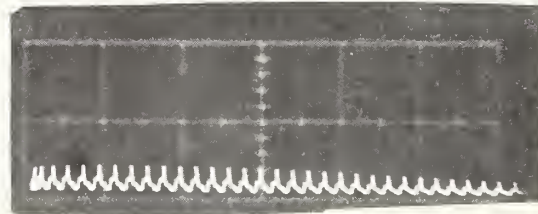
800 J

760 J

610 J

Figure 9   EXCITATION ENERGY DEPENDENCE OF
MODE LOCKING.

9860 dye (T=80%),   100% & 70% mirrors.

42
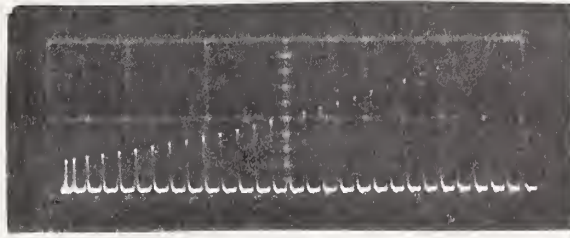
Shot #15
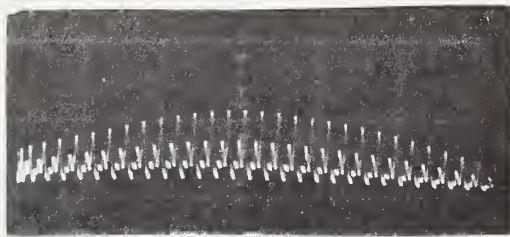
Shot #29
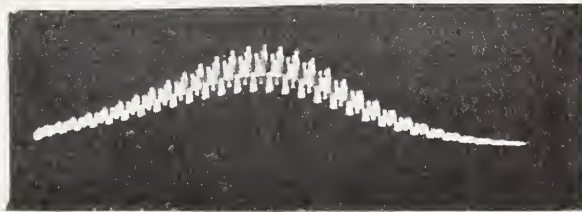
Shot #40

Figure 10   FATIGUE OF DYE.

9860 dye (T=80%),   constant 800 J input.

43
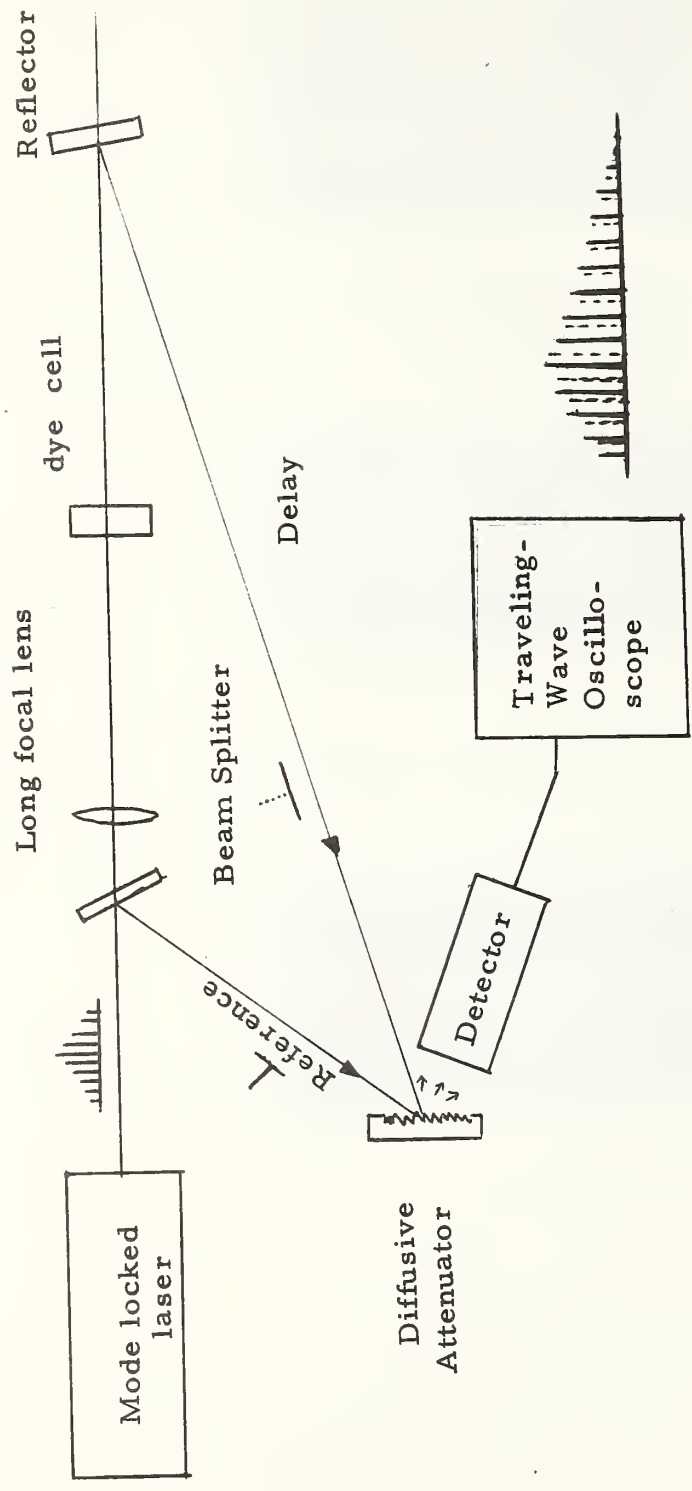
Figure 11 MEASUREMENT OF INTENSITY DEPENDENCE

OF TRANSMISSION OF 9860 DYE.
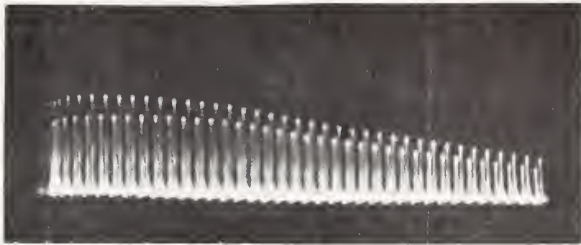
Strong Focusing :
(high power density)
less absorption
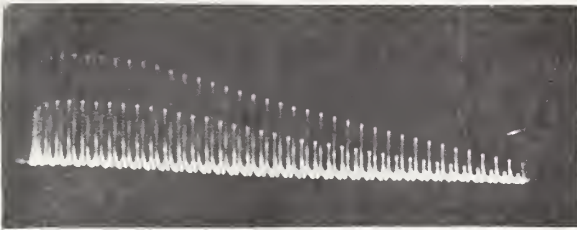
Weak Focusing:
(low power density)
more absorption

Figure 12   OPTICAL ATTENUATION VERSUS INTENSITY
OF 9860 DYE   (T=6%).

45
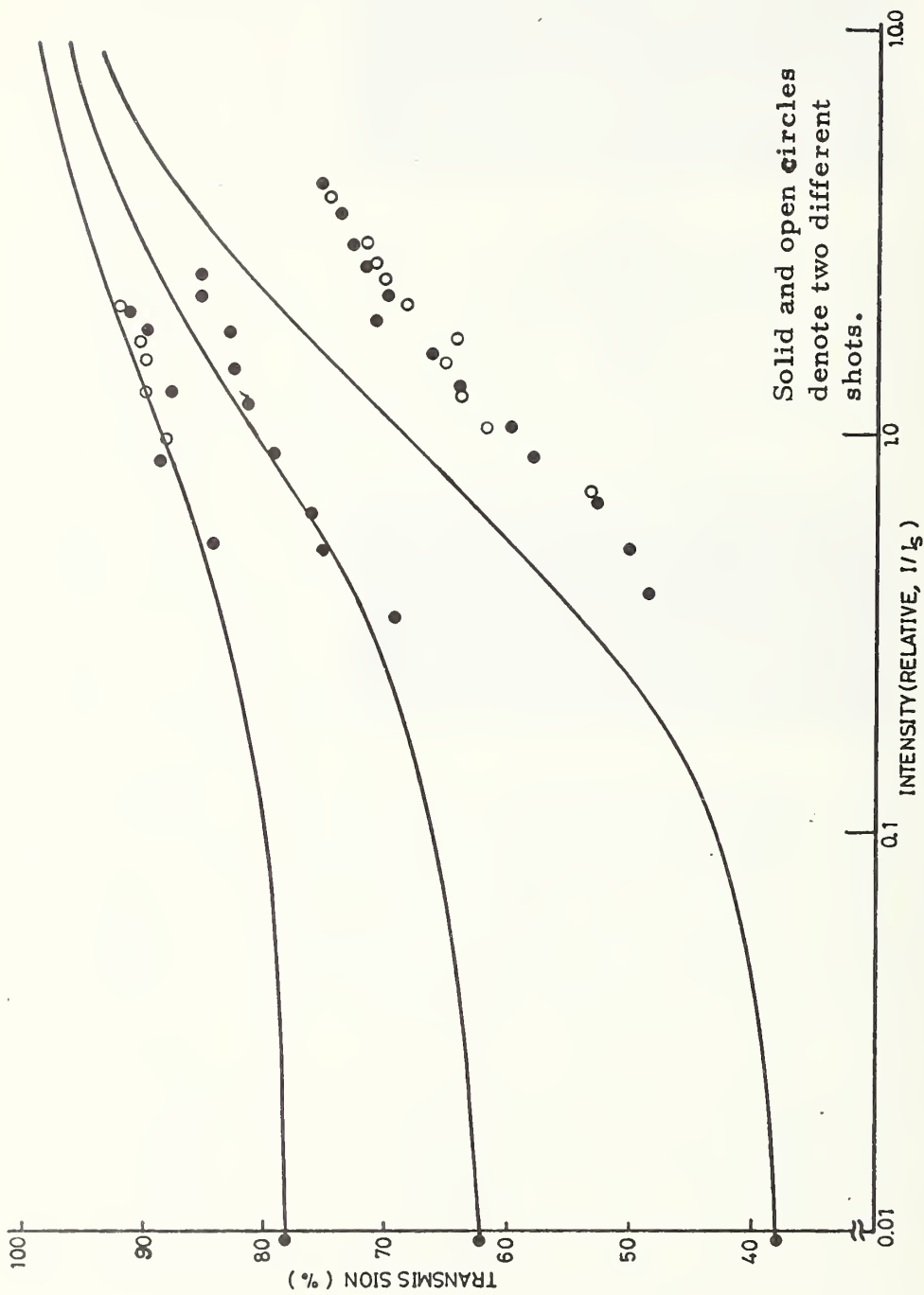
Figure 13   TRANSMISSION PROPERTY OF 9860 DYE.

Solid and open circles denote two different shots.
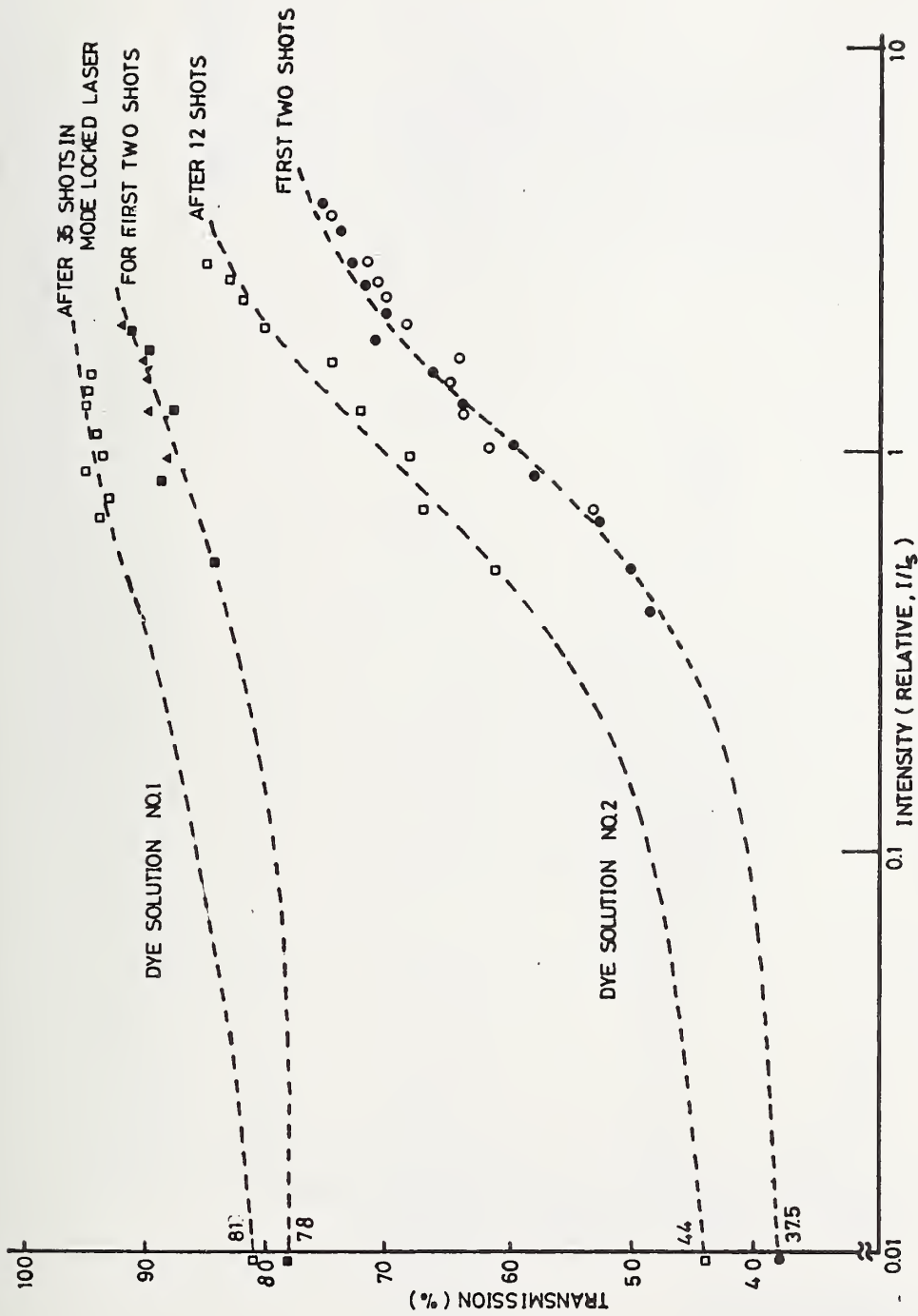
Figure 14 CHANGE OF TRANSMISSION PROPERTY OF 9860 DYE RESULTING FROM MODE LOCKED LASER OPERATION.

47
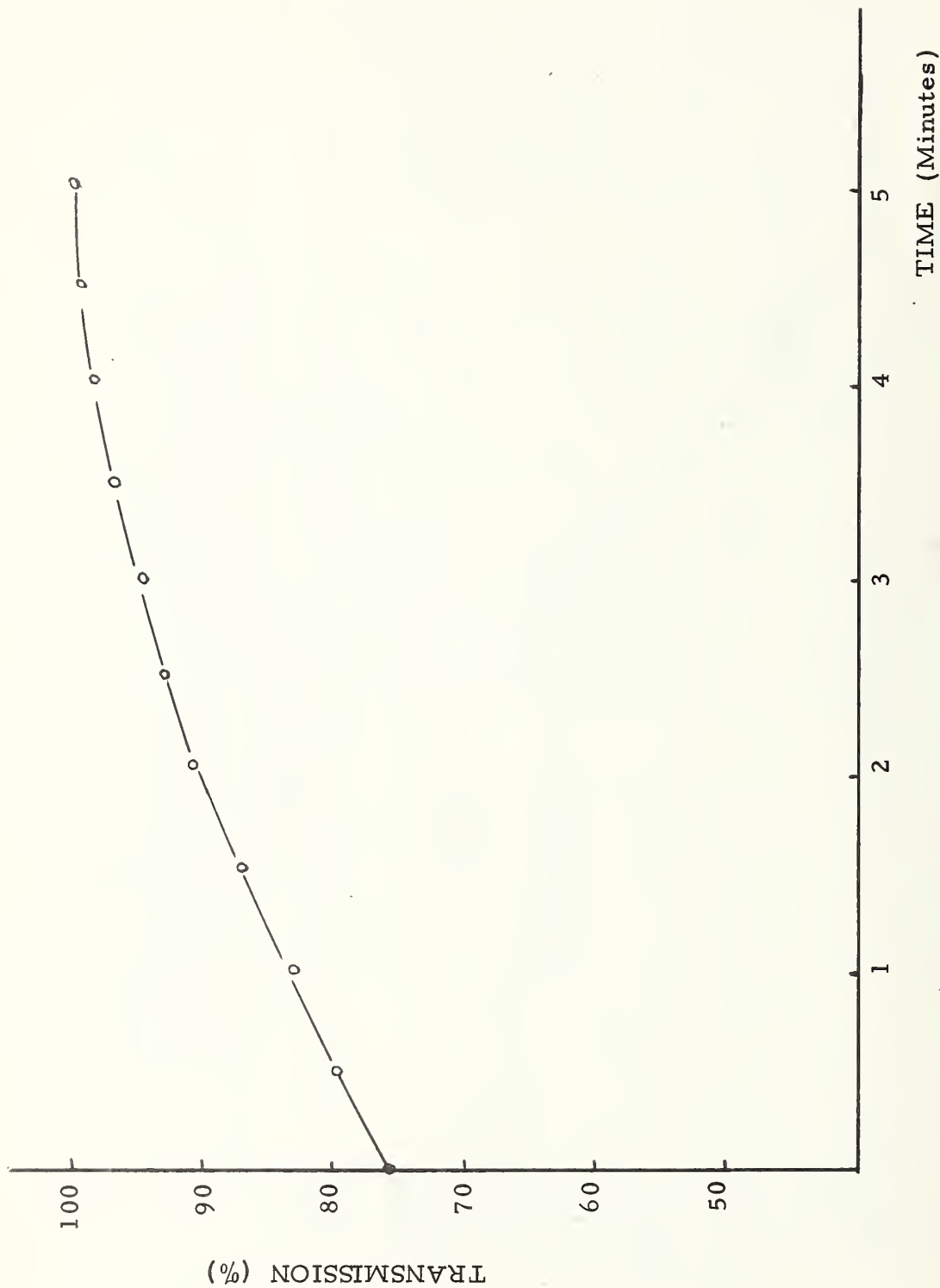
Figure 15 SMALL SIGNAL TRANSMISSION OF 9860
DYE VERSUS EXPOSURE TIME UNDER BLUE LIGHT.

48
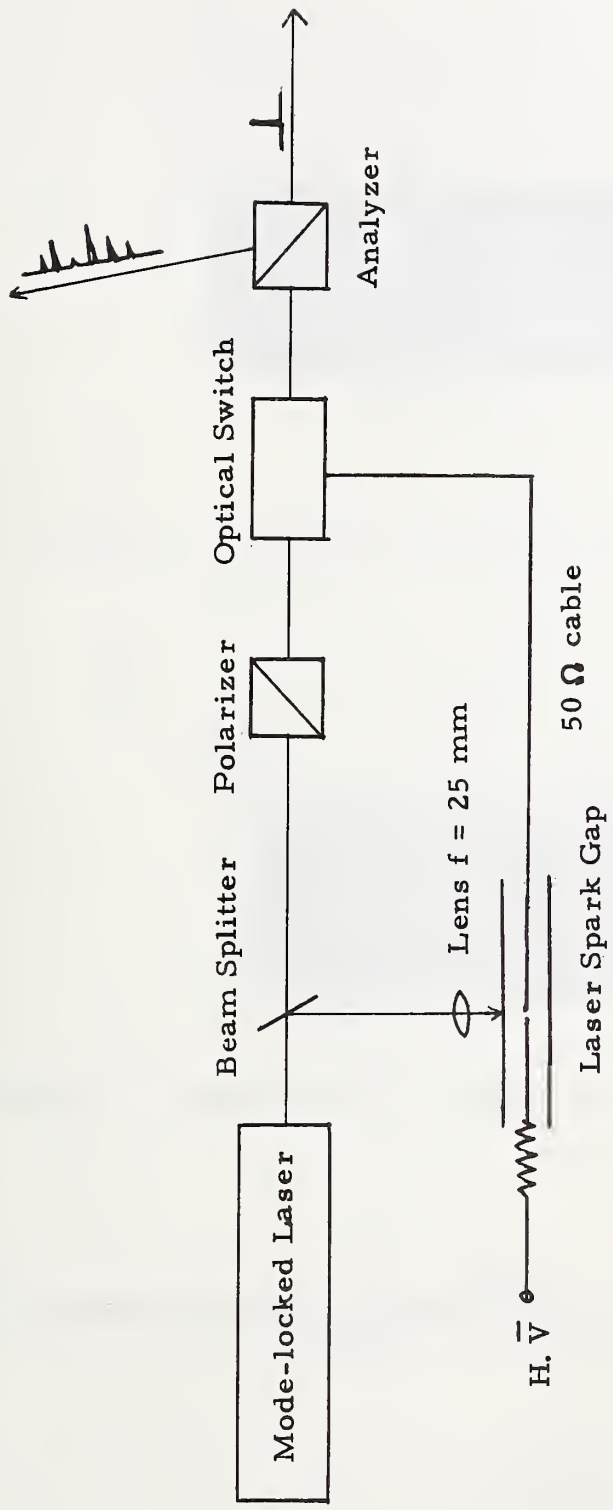
Figure 16 SINGLE PULSE EXTRACTION TECHNIQUE

49
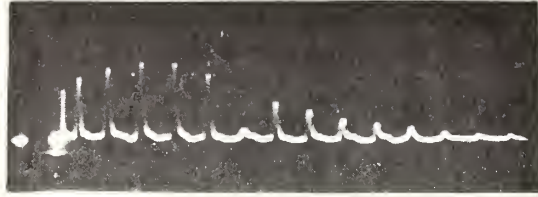
(a) A train of pulses missing a single pulse.   20 ns/div.
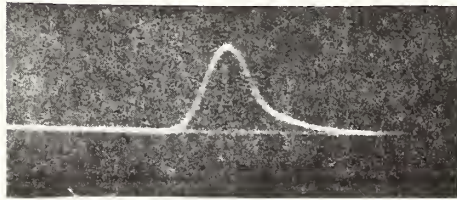
(b) Single pulse extracted from a train of pulses.   5 ns/div.

Figure 17   SINGLE PULSE GENERATION WAVEFORM
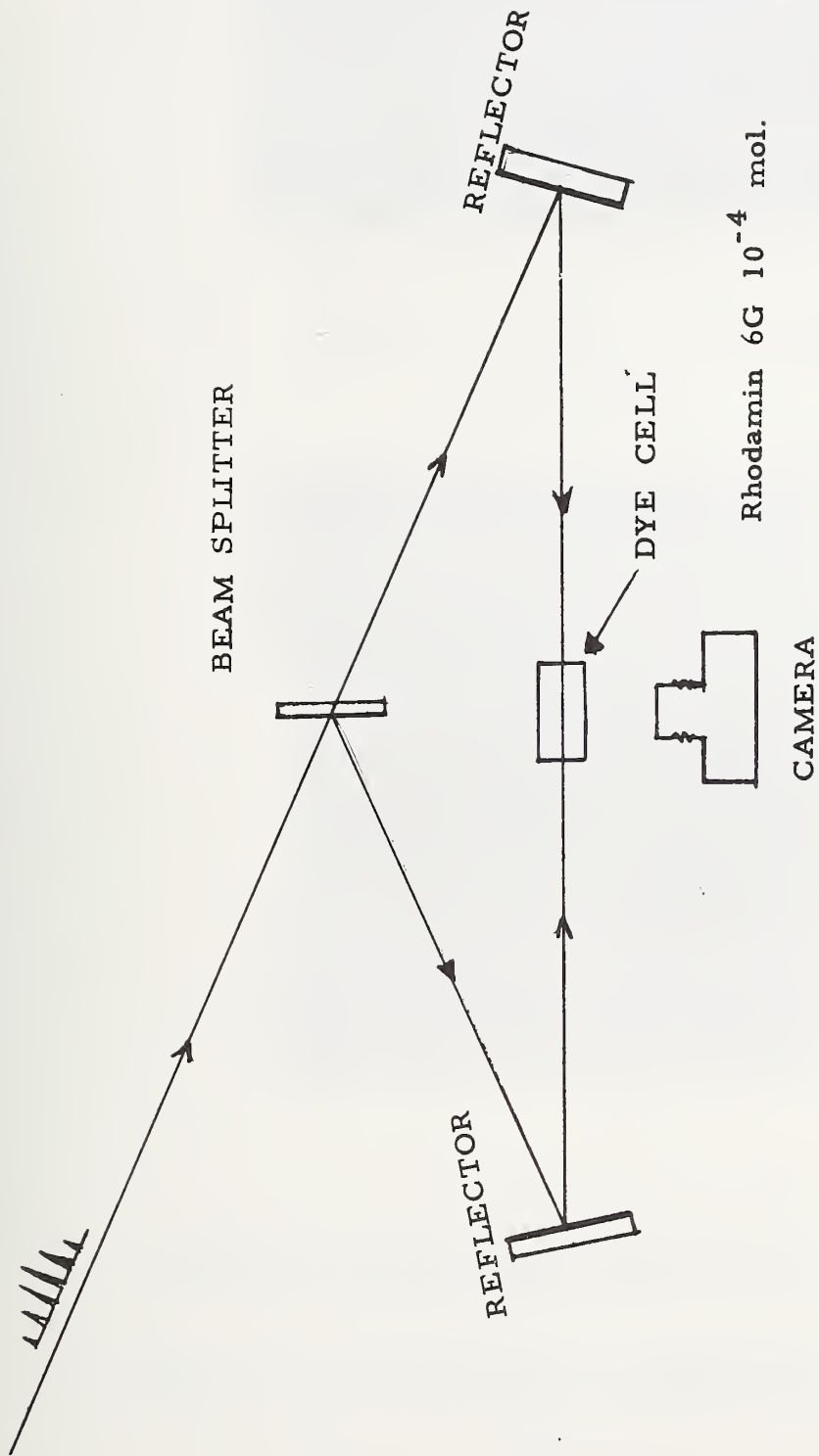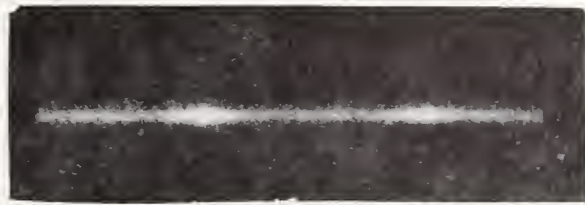
Figure 18   TWO PHOTON FLUORESENCE EXPERIMENTAL
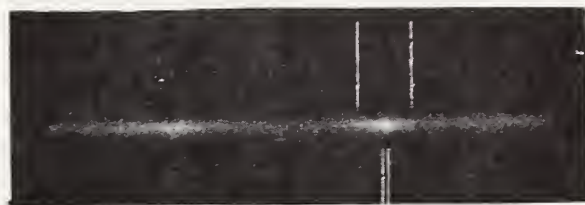SETUP.

51

185 ps

TPF Pattern
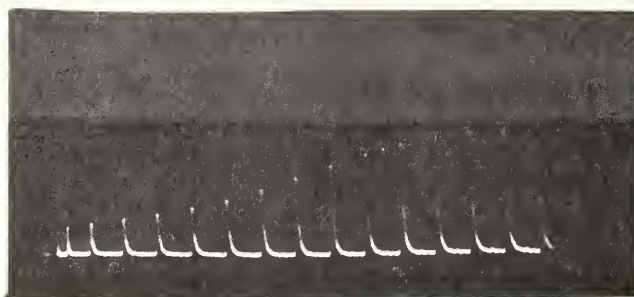
Pulse Wavetrain
20 ns/div.
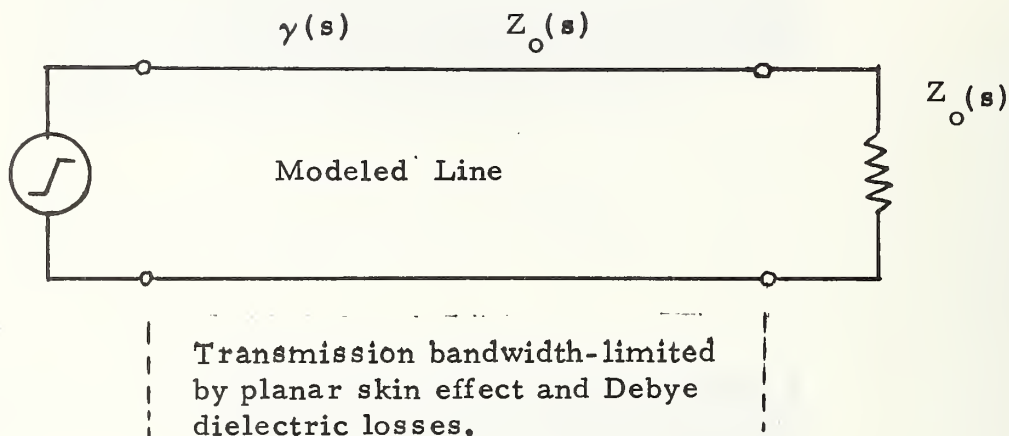
Figure 19   TWO PHOTON FLUORESENCE RESULTS.

185 ps

20 ps

2 ps

Figure 20   TWO PHOTON FLUORESENCE RESULTS.

53

Unit ramp
generator

$\gamma(s)$ $Z_o(s)$

$Z_o(s)$

Modeled Line

Transmission bandwidth-limited
by planar skin effect and Debye
dielectric losses.

(a)   Present NBS reference waveform generator.

Mode Locked
Nd^{+3} Glass
Laser

Measurement
on Pulse
Duration

Modeled
Detector

Impulse response
(Transfer function)
to be predictable
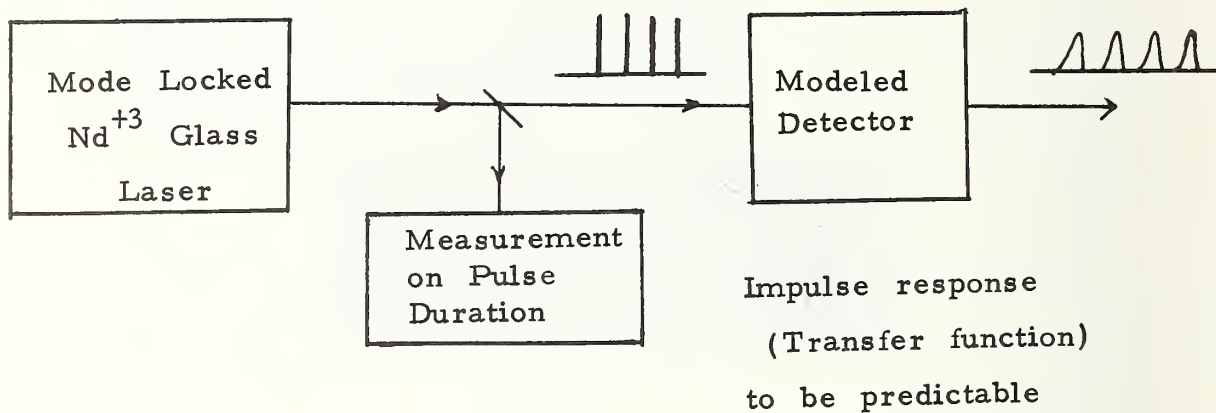
(b)   Proposed future NBS reference waveform generator.

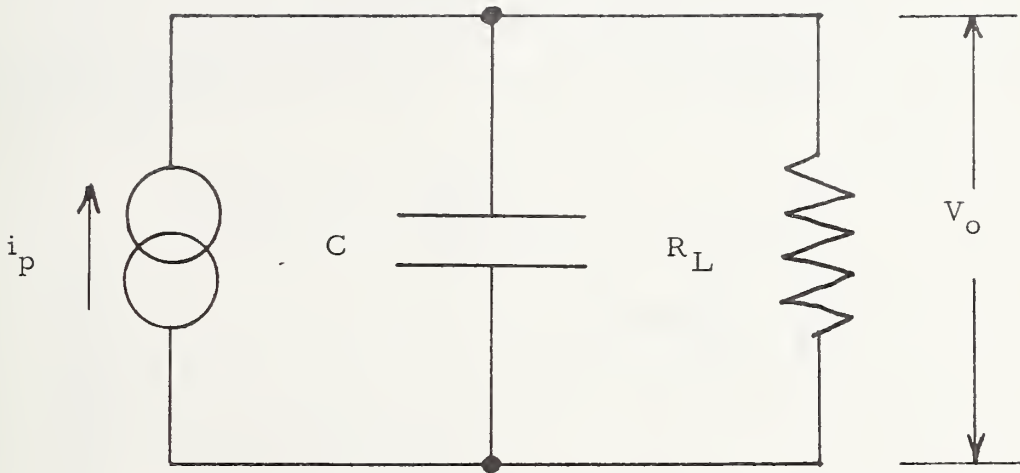Figure 21   GENERATION OF PICOSECOND PULSED
WAVEFORM OF KNOWN SHAPE.

Figure 22   EQUIVALENT CIRCUIT FOR A PYROELECTRIC
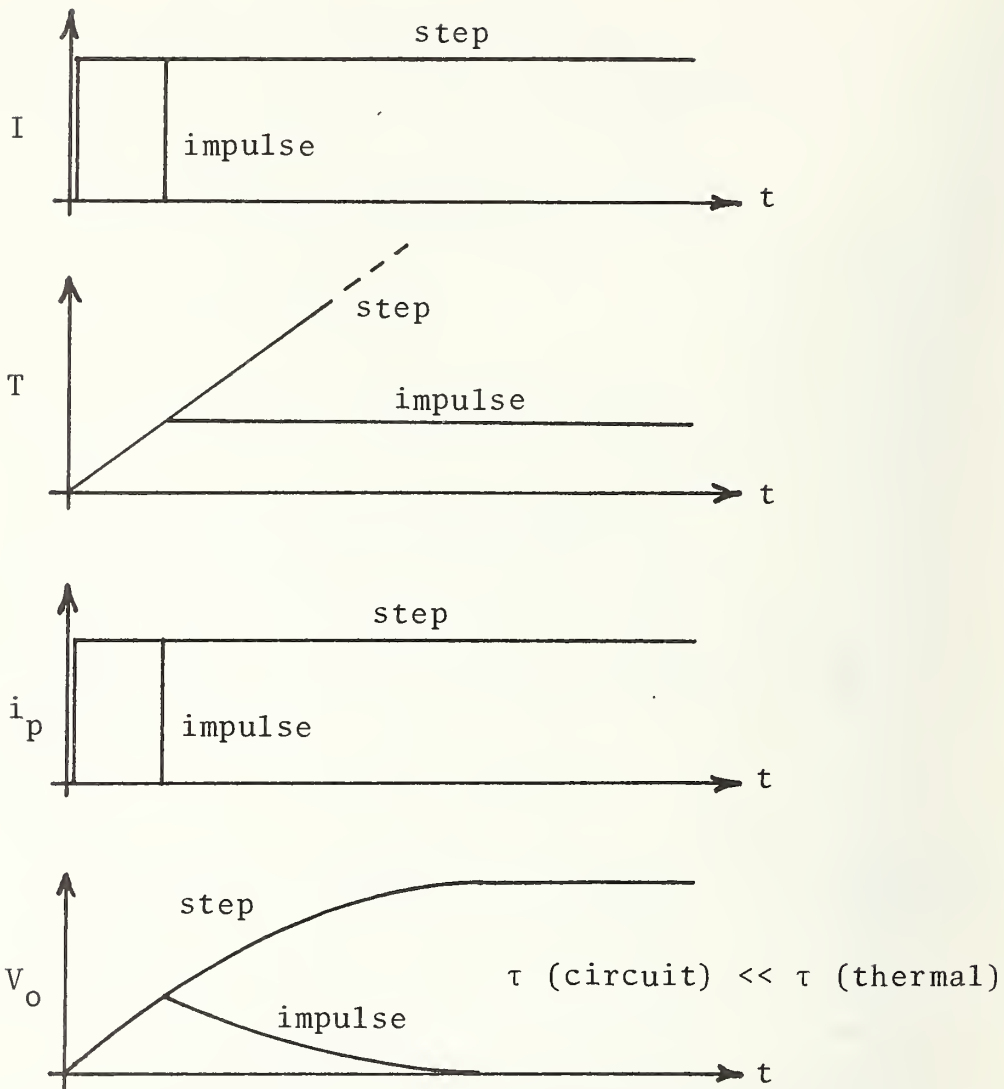   DETECTOR.

55

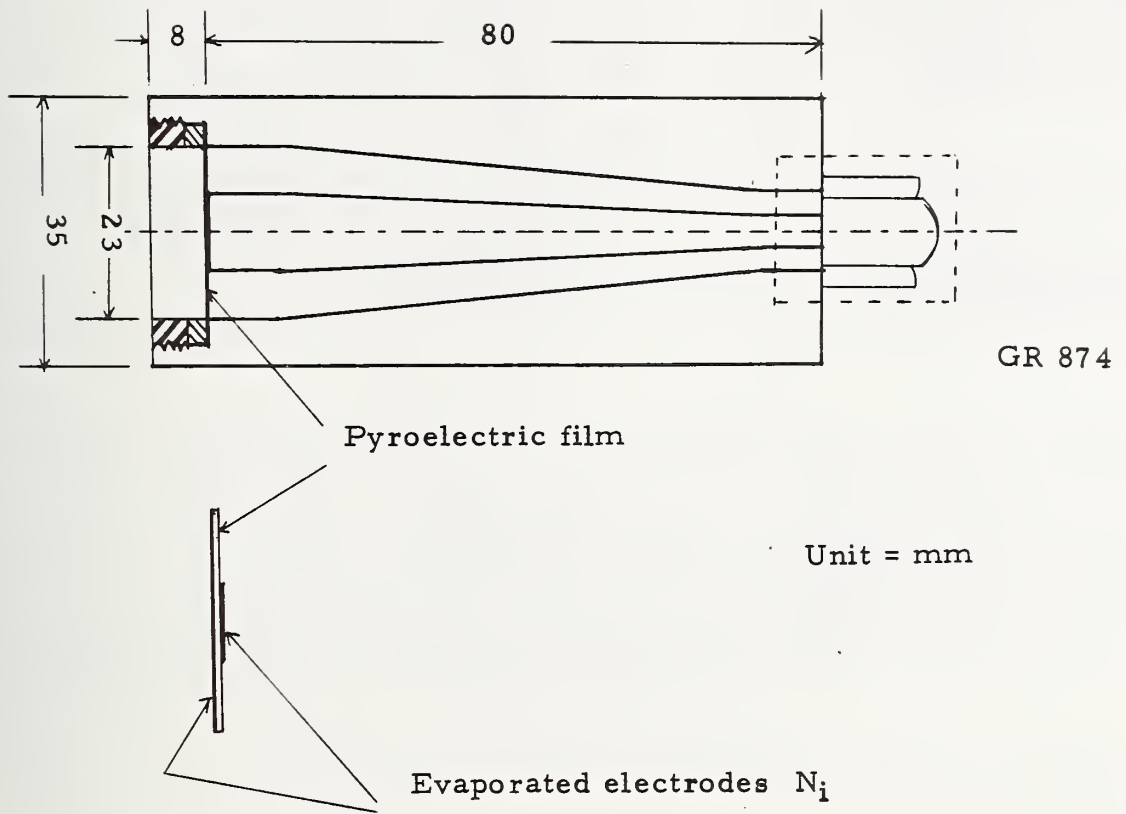Figure 23   PYROELECTRIC DETECTOR WAVEFORMS.

56

8

80

35

23

GR 874

Pyroelectric film

Unit = mm

Evaporated electrodes N_i

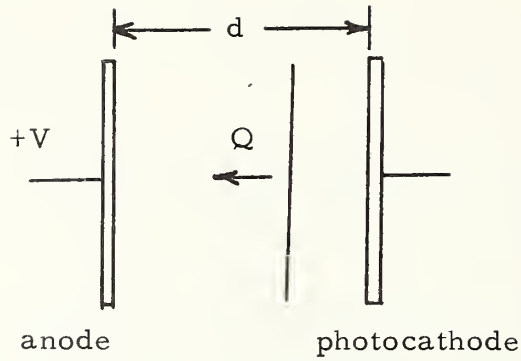Figure 24   PYROELECTRIC DETECTOR.
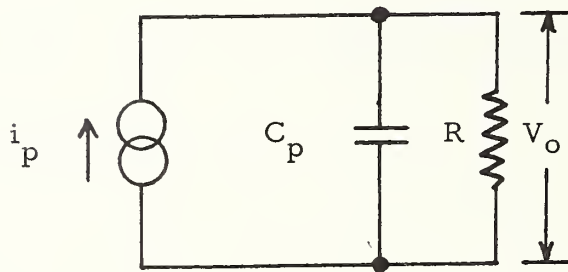
57

Figure 25   BIPLANAR PHOTODIODE.

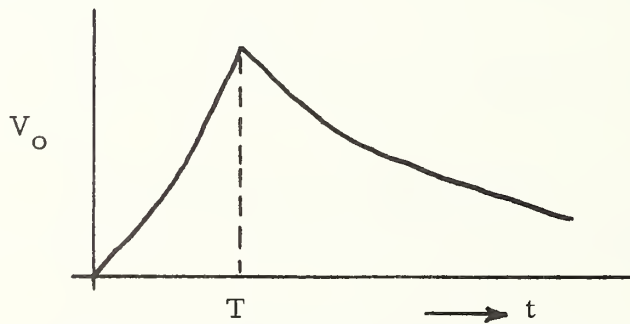Figure 26   EQUIVALENT CIRCUIT FOR BIPLANAR
PHOTODIODE.

Figure 27   IMPULSE RESPONSE OF BIPLANAR PHOTODIODE.

U.S. DEPT. OF COMM. BIBLIOGRAPHIC DATA SHEET	1. PUBLICATION OR REPORT NO. NBSIR 74-360	2. Gov't Accession No.	3. Recipient's Accession No.

4. TITLE AND SUBTITLE	5. Publication Date
A Dye Mode-Locked Nd^{+3} Glass Laser for Generating Electrical Reference Waveforms	September 1972
	6. Performing Organization Code

7. AUTHOR(S) T. Honda and N.S. Nahman	8. Performing Organization

9. PERFORMING ORGANIZATION NAME AND ADDRESS	10. Project/Task/Work Unit No. 2722169 & 2725169
NATIONAL BUREAU OF STANDARDS, Boulder Labs. DEPARTMENT OF COMMERCE Boulder, Colorado 80302	11. Contract/Grant No.

12. Sponsoring Organization Name and Address	13. Type of Report & Period Covered
National Bureau of Standards Department of Commerce Boulder, Colorado 80302	NBSIR FY 72
	14. Sponsoring Agency Code

15. SUPPLEMENTARY NOTES

16. ABSTRACT (A 200-word or less factual summary of most significant information. If document includes a significant bibliography or literature survey, mention it here.)

The theory, design, construction, operation and stability of dye mode-locked Nd^{+3} glass laser are discussed. Optical properties of a saturable dye, single pulse generation and two-photon fluorescence are experimentally studied. For the application of picosecond optical pulses to the field of the baseband pulse measurements, three types of modelable detectors are described which have possible applications for the generation of electrical reference waveforms.

17. KEY WORDS (Alphabetical order, separated by semicolons)
Glass laser; laser; mode-lock; Nd^{+3}; picosecond; reference waveform

18. AVAILABILITY STATEMENT	19. SECURITY CLASS (THIS REPORT)	21. NO. OF PAGES
☐ UNLIMITED.	UNCLASSIFIED	
☒ FOR OFFICIAL DISTRIBUTION. DO NOT RELEASE TO NTIS.	20. SECURITY CLASS (THIS PAGE)	22. Price
	UNCLASSIFIED	